Tailoring of Rail Surface Properties by Laser Surface Modification

FY1995-1996 Report to the Association of American Railroads

J.M. Kramer[†], R.J. DiMelfi[†], K. H. Leong[‡], and B. Hunter[‡]

Argonne National Laboratory
Argonne, IL 60439

[†]Reactor Engineering Division
[‡]Technology Development Division

TABLE OF CONTENTS

I. Introduction 2
- I.1. Railroad Issues 2
- I.2. Approach 2
- I.3. Background 3

II. Experiments 5
- II.1 Laser Treatments 5
  - II.1.1. Facilities 5
  - II.1.2. Nd:YAG Treatments 5
  - II.1.3. CO_2 Treatments 6
- II.2. Microstructural Examination 8
  - II.2.1. Nd:YAG Treated Samples
  - II.2.2. CO_2 Treated Samples 8
- II.3. Friction and Wear Measurements 8

III. Results and Discussion 9
- III.1. Microstructure 9
  - III.1.1. Nd:YAG Treated Samples 9
  - III.1.2. CO_2 Treated Samples 11
- III.2. Friction and Wear 15

IV. Conclusions 21

V. Future Work 22
- V.1. Nd:YAG Laser Treatments 22
- V.2. Friction and Wear Measurements 22
- V.3. Summary of Recommendations for Future Work 23

References 24

I. Introduction

I.1 *Railroad Issues*

The railroads can achieve significant operational and economic benefits by controlling the friction forces at the wheel/rail interface. In general, the ideal condition would be to have high frictional forces on the tread in order to maximize tractive effort, while at the same time to have low frictional forces on the gage face of the rails. Low friction on the gage faces helps minimize flange and rail wear, reduce fuel consumption, and decrease the likelihood of derailments caused by flange climb and low-rail rollover. The present method used to control the friction between the rail and wheel surfaces is to lubricate the side of the rail with greases or oils. These lubricants are applied either by a lubricator mounted on the locomotive or by a trackside lubricator that is activated by the passing of the axles. Both of these methods suffer from uneven application, and the first one is effective only for the locomotive and the first few cars. Furthermore, spreading of the lubricants to the tread reduces traction, which can be detrimental to the operation of the train. Other disadvantages of present lubrication methods include the difficulty in keeping the lubricators operating, and site contamination and environmental concerns.

The desire for improved methods of controlling rail friction and wear has led the railroads to seek a more reliable solution through the use of solid coatings and/or selective modification of the rail surface. In order to be practical, such a coating would have to be capable of reducing the coefficient of friction on the gage faces by a factor of three to five (i.e., a reduction in the nominal coefficient of friction of dry rail from 0.5 down to about 0.1). It would also have to be able to withstand the severe loading and environmental extremes of railroad service without premature failure through spalling, flaking, or corrosion. In addition, the coating will have to be capable of being applied in the field in order to give the greatest latitude for selective application in turns, and for re-application after a period of service or after rail grinding operations.

I.2 *Approach*

It is evident from the above discussion that developing a cost-effective method of controlling friction and wear by modifying the rail surface itself would provide an ideal solution to an array of surface and sub-surface problems in rails. Through appropriate treatment, the friction and wear behavior of steel rails can be tailored in accordance with service requirements. By altering the rail surface microstructure and/or composition, the friction coefficient can be reduced or increased as needed. Reducing wheel/rail friction stresses can reduce wear and the shear component of the service load, which contributes to the nucleation of sub-surface shell defects in the rail [1]. When this is accomplished via direct surface modification of the rail, as opposed to using liquid lubricants, there are the added advantages of not exposing the environment to hazardous chemicals and of not having the lubricating effect "washed away". It is also possible to produce an *increased* friction coefficient via a different modification of an appropriate rail surface. This can improve traction efficiency where needed. These opposing beneficial effects produced by direct rail surface modifications are inconceivable through the use of liquid lubricants. In the context of current technologies, direct surface modification can be achieved in two ways: (1) thermal spraying of appropriate materials onto rail surfaces, and (2) laser treatments of the rail surface, including laser glazing and laser cladding.

Laser surface modification offers unique advantages to the user because of the ability to apply high local energy fluxes to the part surface while keeping the total heat input low. The controlled, localized application of energy keeps the bulk of the part cool enough to act as a heat sink during the treatment. This integral heat sink results in very steep temperature gradients and large cooling rates which allow the surface to be modified and then "frozen" in the desired metallic state. We believe that laser surface treatments produce a more blended transition between surface and substrate, and hence provide a stronger, higher-integrity interface than that produced by thermal spray treatments. Therefore, we are investigating the feasibility of laser surface modification of rails as a means to address some of issues of concern to the railroad industry.

I.3 ***Background***

This project year (FY95-96), we focused on proving the principle that a suitable laser treatment could serve to reduce the friction and wear of a steel rail surface. Sliding friction on macroscopically smooth metal surfaces (steel wheels on rails), under loads sufficient to deform or fracture microscopic asperities, is usually associated with the work expended in deforming the materials plastically and/or fracturing them. Wear of strong ductile metals like rail steels is associated with the plastic-flow induced build-up of strength gradients in the subsurface region and the deposition of deformation related defects in subsurface layers. This creates interfaces parallel to the surface along which separation occurs leading to material removal (wear) after many cycles of loading. Hence, in this class of materials, friction and wear are related to each other through the propensity for plastic flow, and one often finds that a reduction in one is accompanied by a reduction in the other. Lubricants provide interlayers between surfaces that allow one to slide past the other more easily without forcing deformation, and in some cases they inhibit the formation of bonds between asperities that then must be fractured for sliding to continue. Without lubricants, friction and wear of smooth surfaces can be mitigated by changing them in a way that limits plastic flow, i.e. by making them harder. Hard materials are often observed to have low friction coefficients. For example, single crystal diamond has the lowest coefficient of friction found in nature.

To maintain the toughness and relative inexpensiveness of rail steel while reducing wheel/rail friction, an ideal approach is to modify the loading surface of existing rail in a way that renders it substantially harder yet leaves the substrate unaffected. Laser treatments can accomplish this [2] by changing the surface microstructure, and doing so in a such a way that the surface layer undergoes a smooth transition into the substrate and is well bonded to it. Modifications can be enhanced by distributing another substance (cladding) on the surface during or before laser treatment. One way to harden the surface of rail steel is by simply heat-treating it with the laser: i.e. heating it in the solid state to the austenitizing temperature and allow it to cool rapidly to form hard martensite. The hard surface layer will resist plastic flow and reduce friction and wear. This simple process has some minor disadvantages. Unlike in the case of hard bulk materials, like diamond, a thin hard surface when loaded substantially will transmit these loads to the soft substrate, which can deform even if the surface does not. If the surface layer has the same elastic modulus as the substrate, as is the case with martensite, it cannot mitigate stress concentrations any differently than an untreated surface. However, a surface layer with a smaller modulus than the substrate can distribute these concentrations elastically within the layer and mitigate their effect on the substrate. Also, if the

martensite surface layer does deform plastically, it will do so in the same manner as untreated rail steel, producing a damage layer along which separation can eventually occur leading to delamination. What is needed then is a surface layer that is hard with respect to plastic flow, is elastically compliant, and, when it does deform plastically, does not produce a damage layer. Laser glazing can be an ideal treatment to achieve this goal. One can include a cladding material with this process for additional lubricating benefits, if necessary.

In laser glazing, a thin surface layer is melted and rapidly solidified to produce an amorphous [2] or quasi-amorphous surface film. The lack of crystalline order in such materials makes them substantially resistant to plastic flow [3], and hence very hard. They generally exhibit about a 30% or greater reduction in elastic modulus. If they do deform plastically, localized defects are not involved, and the more open structure tends to be self healing. Consequently, repeated plastic flow is less likely to result in debris being deposited in a subsurface damage layer. For these reasons, the laser glazing process alone may be sufficient to provide satisfactory reductions in friction and wear. This process has been studied by several researchers [4-7] over the years and applied to many materials, including the kinds of steels of interest to the railroads. These studies often include the consideration of simultaneous application of cladding materials [8] as part of the glazing process. Very recently [9], work has been done to simulate the effects numerically of laser hardening of carbon steels. Understanding these effects is still the subject of ongoing research. However, the properties observed and calculated for treated surfaces are promising with regard to the goals of this project.

With regard to utilizing this technique for railroad applications, it should be noted that equipment sufficient to the task is readily obtainable. High-power lasers are commercially available from many vendors and at different power levels. CO_2 lasers, which operate at a wavelength of 10.6 μm, offer the highest total power. Typical production lasers deliver 3-10 kW, although higher power lasers capable of delivering more than 40 kW (often for specific tasks) are available. These lasers are typically continuous wave (CW) in nature, although various pulsing modes and schemes are available. Pulsing is not required for heat treatment. Nd:YAG lasers, which operate at a wavelength of 1.06 μm, are available in configurations capable of delivering up to 3 kW. The 2-3 kW lasers have become available only in the last few years. Like the CO_2 lasers, Nd:YAG lasers are available in pulsed and CW versions.

This year, we have explored the efficacy of using the process of laser glazing, primarily without cladding, to mitigate friction and wear for the level of loading magnitudes of interest to the railroads. We bring to the project experience in studying the friction and wear behavior of amorphous films on crystalline substrates for carbon steels [10]. It was observed that such films, produced by ion implantation [11], can reduce the friction coefficient by a factor of three. It was shown that this kind of improvement in properties can be accounted for by the behavior of the amorphous film on crystalline substrate morphology. We also bring considerable experience in laser treating surfaces. Over the last few years, staff at Argonne National Laboratory's Laser Applications Laboratory (LAL) have carried out experiments aimed at optimizing processes and demonstrating novel techniques for laser surface modification. Success depends upon understanding the various interaction regimes of

the laser and the metal. These interaction regimes are delimited by irradiance and interaction time conditions. With appropriate choices of laser power, irradiance profile and interaction time, successful surface modification can be effected on large or small parts, in bulk conditions or near part edges, and on low (e.g. 1020 steel) or high (e.g. 1045, 1080 steel and ductile iron) carbon content materials.

For some processes Nd:YAG is preferred over CO_2. Traditionally, Nd:YAG required less maintenance because it is a solid-state laser. However, new sealed CO_2 systems have significantly reduced the maintenance and consumables requirements. Although Nd:YAG systems are not available with as much power as large CO_2 lasers, there are significant differences in the absorptivity of metals at these two wavelengths. Under conditions typical of heat treatment, only about 10% of the CO_2 energy incident on a bare metal surface is absorbed (hence the requirement for coatings which raise the absorptivity to greater than 80%). The shorter Nd:YAG wavelength results in absorptivity of 35-50% on bare metal, which makes it possible to heat treat, glaze, and clad without an absorptive coating. With a coating, CO_2 and Nd:YAG have about the same absorptivity. The absorptivity of a bare metal surface increases with surface roughness.

II. Experiments

II.1. *Laser Treatments*

II.1.1 . Facilities: Staff at the Laser Applications Laboratory carry out research and development on laser-based applications for materials processing and aerosol or spray characterization. Collaborative research and development activities with industrial partners are a key activity. An integrated approach maximizes the synergy between laser and beam delivery manufacturers, and technology developers and users.

The LAL facility houses two high-power industrial laser systems complete with diagnostics for materials processing functions: a 6 kW Rofin-Sinar RS6000 CO_2 laser and a 1.6 kW Electrox pulsed Nd:YAG laser. Both laser systems have CNC-controlled 4 or 5-axis workstations. The equipment was provided by a $1.7 million grant from the State of Illinois for Argonne and industrial partners to develop advanced material processing methods. The capabilities include cladding, cutting, drilling, heat treating, welding and laser thermal simulation studies. The general goal of the laser processing effort is to optimized laser processing parameters for materials processing functions.

II.1.2. Nd:YAG Treatments: An initial test for proof-of-concept purposes was done using a piece of virgin rail. The rail was used as-is, except for having the rust removed from the surface. The surface was still somewhat rough, which served to enhance coupling of the Nd:YAG laser beam energy into the rail.

The optics used were a 77 mm EFL spherical BK7 plano-convex lens placed on top of a 5"cylindrical BK7 plano-convex lens. These lenses were used to produce an astigmatic, defocused beam with an oval profile. The major and minor axes of the oval are 10 mm and 4.4 mm; at the 86% energy enclosure intensity levels, the major and minor axes are 4.2 mm and 3.6 mm. Generally, the 86% energy enclosure levels correspond to the effective width for heat treatment. The intensity profile of the beam (measured at a lower average energy) is depicted in both false color and isometric views in Figure 1 and Figure 2.

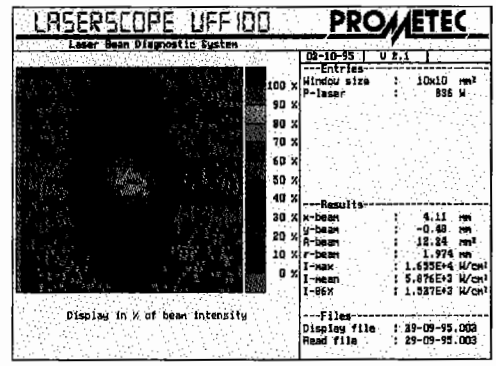

Figure 1: False color depiction of intensity profile.

The laser parameters used were set for a peak power of 4 kW, a pulse length of 2 ms and a pulse rate of 200 Hz. This resulted in a delivered average power of 1150 W and a delivered peak power of 2.88 kW.

Five passes were made at different speeds: 2.0, 1.5, 1.0, 0.75, and 0.5 cm/s (47.2, 35.4, 23.6, 17.7, and 11.8 inches/min). This range of speeds provided surfaces that ranged from a standard heat treatment to a deep surface melt. Samples from these tracks were identified as YAG1, YAG2, YAG3, YAG4, and YAG5, respectively.

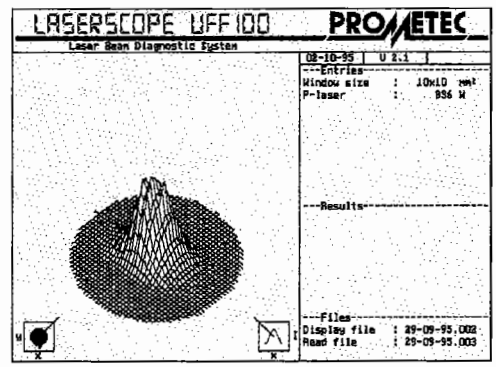

Figure 2: Isometric depiction of intensity profile.

II.1.3. <u>CO_2 Treatments</u>: A follow-up test was conducted using a CO_2 laser. The CO_2 laser's greater power made it possible to glaze a wider track for friction and wear tests. A beam scanner (Spawr Industries) was used with the mirrors configured so that a 9 mm long line source was rastered across an 8 mm wide region. The gas flow rates were 70 cfh of N_2 through the cross jet and 2 lpm for protection of the weld sensor. The delivered energy yielded an effective sinusoidal intensity profile (hot edges).

The surface of the rail was divided into three sections: one coated with a proprietary inert coating, one coated with flat black Krylon paint, and one bare. The inert coating and paint sections were coated until visually uniform and the metal appeared covered. For the inert coating, this typically results in a coating thickness of 1.5-2.0 mils. For the Krylon, the paint thickness is typically 0.3-1.0 mils using this technique. The coatings were allowed to dry for about three hours.

Based on scoping tests with bare, painted, and inert coated 3/8" thick 1045 steel plates, processing parameters were agreed upon based on visual examination of the 1045 steel plates. Initial tests were conducted on a 3" rail segment. The inert coating section was glazed at 0.42 cm/s (10 inches/min). The painted section was glazed at 0.34 cm/s (8 inches/min). For both of these runs the

conical power puck recorded the delivered power to be 2300 W. The surfaces were visually smooth, although inspection under magnification revealed some micro-craters. The attempt at glazing the bare section was at 0.97 cm/s (23 inches/min) and 4200 W. Metallographic and friction samples cut from the 3" (short) rail along the Krylon painted track were labled with the prefix SB; those taken from the inert white coated track were labled SW; and those taken from the bare metallic track labled SM.

Repeat tests were carried out on a 7" rail segment, although the glazing only used a 3" length, so that additional segments would be available for reference or later use. The parameters were altered slightly to provide some additional range of data. The processing speed was reduced to 0.34 cm/s (8 inches/min) for the inert coating and 0.25 cm/s (6 inches/min) for the paint (still at 2300 W). For the bare segment the speed was reduced to 0.80 cm/s (19 inches/min), still at 4200 W. The bare segment glaze was more successful this time. The surface quality of the inert coating and paint were still visually acceptable. Metallographic and friction samples cut from the 7" (long) rail along the Krylon painted track were labled with the prefix LB; those taken from the inert white coated track were labled LW; and those taken from the bare metallic track labled LM.

II.2. *Microstructural Examination*

II.2.1. Nd:YAG-treated Samples: As just indicated, the Nd:YAG treatments were applied to an actual rail-head surface to establish that a suitable glaze could be applied to this material and geometry using commercially available equipment. The range of treatments described above resulted in a number of tracks that clearly showed melting on the surface both to the naked eye and with the aid of low power stereo-microscopy. Samples were cut from these tracks, metallographically mounted in cross-section, polished, and etched with Villela's solution. The near-surface microstructure of these mounted samples was examined in a Nikon Metaphot V Series metallographic microscope. Microhardness measurements were made of the laser-modified microstructures and the substrate regions using a Leitz Miniload 2 microhardness tester.

II.2.2. CO_2 -treated Samples: As described earlier, past experience indicates that this laser often requires that a coating be applied to surfaces like rail steels in order to achieve proper coupling and melting. Figure 3 is a photograph showing the different coatings and the appearance of the different treatments. The bare-metal sample showed some melting, but it was not continuous along the laser track. The samples painted with the white proprietary coating and the black-painted samples gave satisfactory results with regard to melting, based on low-power stereo-microscopic observation. The black painted samples appeared to give the best results at this level of observation. However, because the CO_2 laser had to be "rastered" perpendicular to the direction of the laser track in order to achieve the desired track width, more energy was deposited at the beginning and end of the track width. Consequently, although the extent of melting on these tracks was largely uniform, the most melting appearing at the two extremities of the track width. These samples were metallographically prepared as described above, and microscopically examined. Micro-hardness tests were also performed near the treated surfaces.

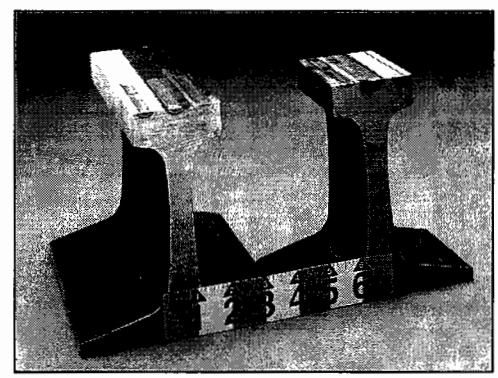

Figure 3: CO_2 -Treated Rail Segments

II.3. *Friction and Wear Measurements*

Two of the key attributes of an effective coating for the gage face of rails are reduced friction and decreased wear. For the subscale testing in the present study, there were several conflicting considerations that went in to the selection of the method used to measure friction and wear of the laser treated rail. On the one hand, it is desirable to use an intact (or nearly intact) rail section for the laser treatment because the results are likely to depend on the thermal mass that is available to produce the rapid cooling that is required. On the other hand, use of an intact rail section for preparing the coatings limits the shape of the test coupons unless elaborate machining techniques are used. As a compromise, simple block test samples where chosen which could easily be cut from

parallel laser tracks that were laid down on the head of a rail that had been machined flat across a 2.5-inch width. The samples conformed to the ASTM G77-93 [12] specifications for the "Block-on-Ring" friction and wear test method.

In the block-on-ring friction and wear test, a test block is brought into contact with a test ring that rotates at a constant speed for a given number of revolutions. The contact force between the block and the ring is set prior to the test. The friction force necessary to keep the block in place is continuously measured. The wear that occurred during the test is determined by either measuring the weight loss of the ring and the block, or, as was done for the present study, measuring the width of the scar left on the block. The depth of the scar can also be estimated by using the scar width and the known radius of the ring (17.5 mm). This result is not precise because there is movement of the block toward the load cell during the test, which tends to widen the scar somewhat.

The standard G77-93 test block is 0.4000 inches (10.16 mm) tall, with the contact surface 0.620 inches (15.75 mm) long and 0.250 inches (6.35 mm) wide. The latter dimension dictated that the laser tracks on the rail sections needed to be at least 0.250 wide. This could not be achieved by a single pass of the Nd:YAG laser, and it was thought that multiple passes could destroy the microstructure that was developed during the previous pass. As noted above, the CO_2 laser is capable of producing an 8 mm track using the beam scanner and, therefore, was chosen for producing the friction and wear test samples.

A block-on-ring test apparatus is not available at Argonne. However, the leading manufacturer of this equipment, Falex Corporation, is located nearby in Aurora, Illinois. Falex also performs testing services on a contractual basis. Consequently, all of the friction tests discussed later in this report were performed by Falex using test conditions that were determined following consultations with Argonne and the Association of American Railroads.

III. Results and Discussion

III.1. *Microstructure*

III.1.1. Nd:YAG-treated Samples: Figure 4 shows the typical near-surface microstructure of the cross-section perpendicular to the laser track of Nd:YAG-treated samples, on which surface melting occurred. The sample shown was etched with Villela's solution. Three regions are evident in the micrograph: a glazed region at the very surface, a heat-affected zone, and the substrate region having the original rail-steel pearlitic microstructure. The heat-affected zone displayed the microstructure typical of untempered martensite. The ten μm-thick glazed region etches differently and does not show the microstructural detail of a crystalline phase. While it is difficult to be sure at this magnification in an optical microscope, we believe that this glazed layer may be an amorphous or quasi-amorphous material having desirable properties with regard to friction and wear.

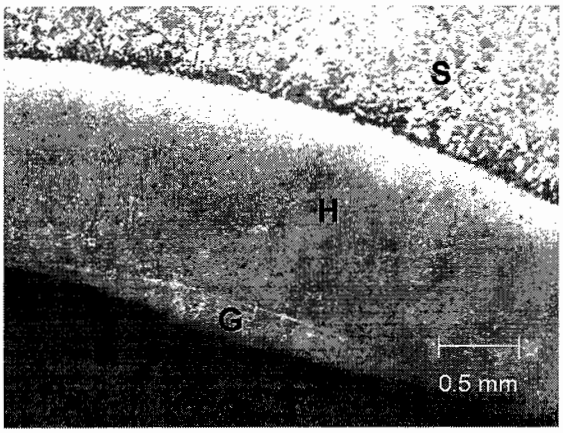

Laser-glazed surface of rail steel sample showing structure of base substrate material (S), heat-affected zone (H) and "glazed" region (G) (etched).

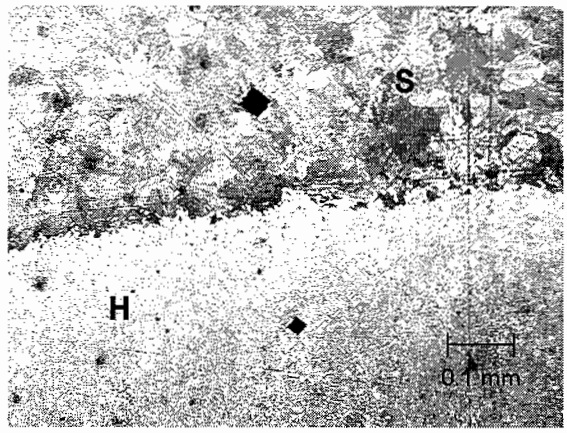

The same sample as on the left showing Vickers hardness impressions in the substrate (HV 300) and the heat-affected zone (HV 840) made at the same load (etched).

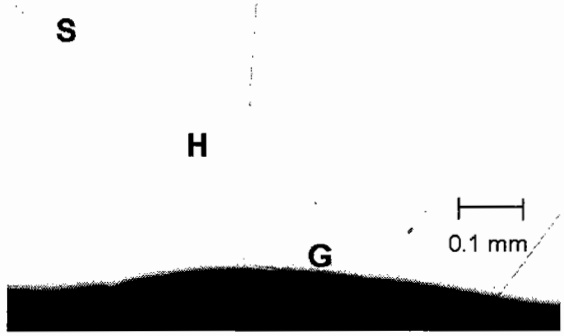

Unetched sample of laser-glazed rail steel surface, showing the high integrity of the interfaces between the substrate, heat-affected zone and "glazed" regions.

Figure 4: Microstructure of Nd:YAG Laser Track in which Melting Occurred.

Microhardness measurements are shown in Table I. The values shown are the average of three readings from three randomly selected areas in the three microstructural regions.

Table I. Vickers Hardness of Laser Treated Samples

Region	**YAG** (Track YAG3)	**CO_2** (Track LB)
Substrate	306	319
Heat-Affected Zone	841	825
Glazed	802	733

The hardness of the glazed region is somewhat less than that of the martensite, but both are substantially greater than that of the substrate region. As discussed earlier, this kind of increase in hardness coupled with the elastic and flow properties of an amorphous material may very well provide us with very much improved friction and wear properties. Unfortunately, the glazed region of Nd:YAG laser tracks on these samples were not wide enough for the standard block-on-ring friction and wear testing. Also, since they were produced directly on an actual rail head, the original surface was curved, which restricted our ability to prepare standard samples. Nonetheless, the hardness results and microstructural observations are promising for this surface treatment.

III.1.2. CO_2 -treated Samples: The width of the laser tracks for this treatment could be controlled by the magnitude of the lateral rastering, so this dimension was chosen to allow us to cut standard friction and wear samples from them. As mentioned above, tracks were applied to unpainted samples, samples painted with commercial flat black paint and samples painted with a proprietary coating (white). In this case the laser was applied to a flat surface machined from an actual piece of virgin rail head. The surfaces of all of these laser-treated samples appeared mottled and pitted to the naked eye and in the low-power stereo-microscope (Fig. 5). This may imply a less satisfactory surface than what was obtained from the Nd:YAG treatments. When viewed in cross-section, these "pits" penetrate through the thickness of the treated surface (Fig. 6). We believe that this may be an unsatisfactory consequence of the CO_2 laser treatment, at least in the way it was applied here. The cross-section microstructure was similar for all the laser-treated samples, showing a heat-effected zone that is typically untempered martensite and a pearlitic substrate. Only the black-painted sample, which seemed to show the most melting, showed a hint of a glazed region at the two hot edges of the laser track produced by the rastering pattern (Fig. 7). The hardness of the different microstructural regions is shown in Table I. Once again, the values shown for each region are the average of three readings. As before, the heat-affected zone and the possible glazed region are substantially harder than the substrate. Therefore this treatment is also promising, but efforts must be made to correct the problem of pitting, and to spread the glazed region across the entire width of the track.

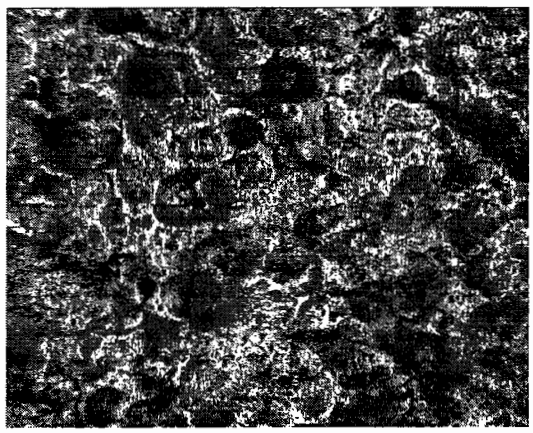

Surface of CO_2 Laser Treated Sample LB2

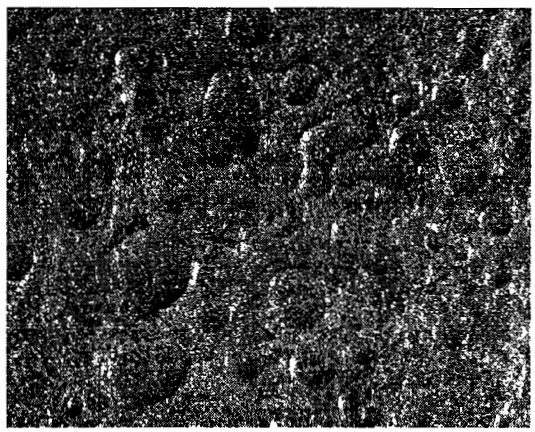

Surface of CO_2 Laser Treated Sample LW2

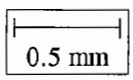

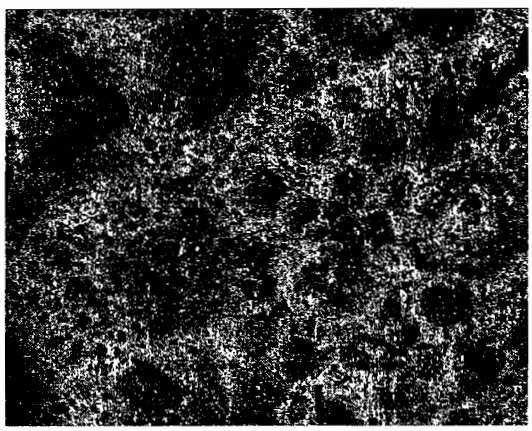

Surface of CO_2 Laser Treated Sample LM2

Surface of YAG Laser Treated Sample YAG3

Figure 5: Surface Pitting of CO_2 Laser Treated Samples in Comparision to YAG Treated Sample

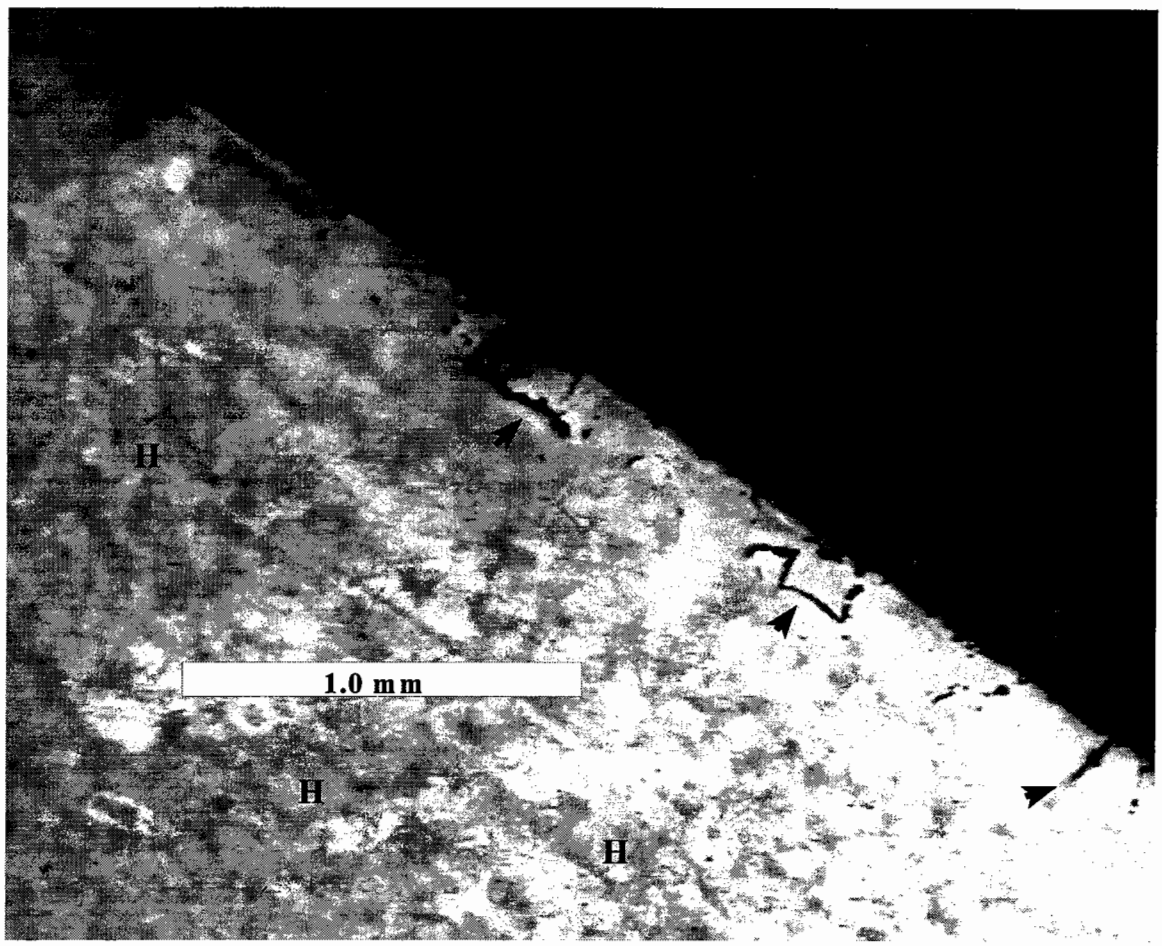

Figure 6: Cross Section of Surface of Sample LB2 Showing Pits (Arrows) in Melted Zone. The adjacent heat-affected zone is denoted by areas labeled "H".

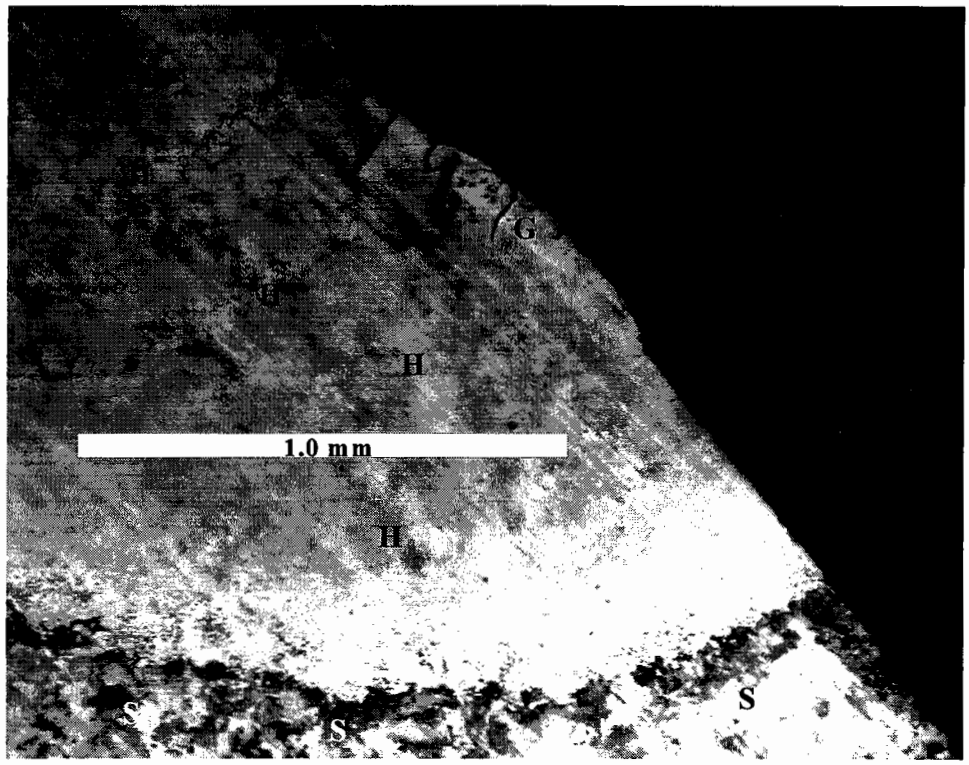

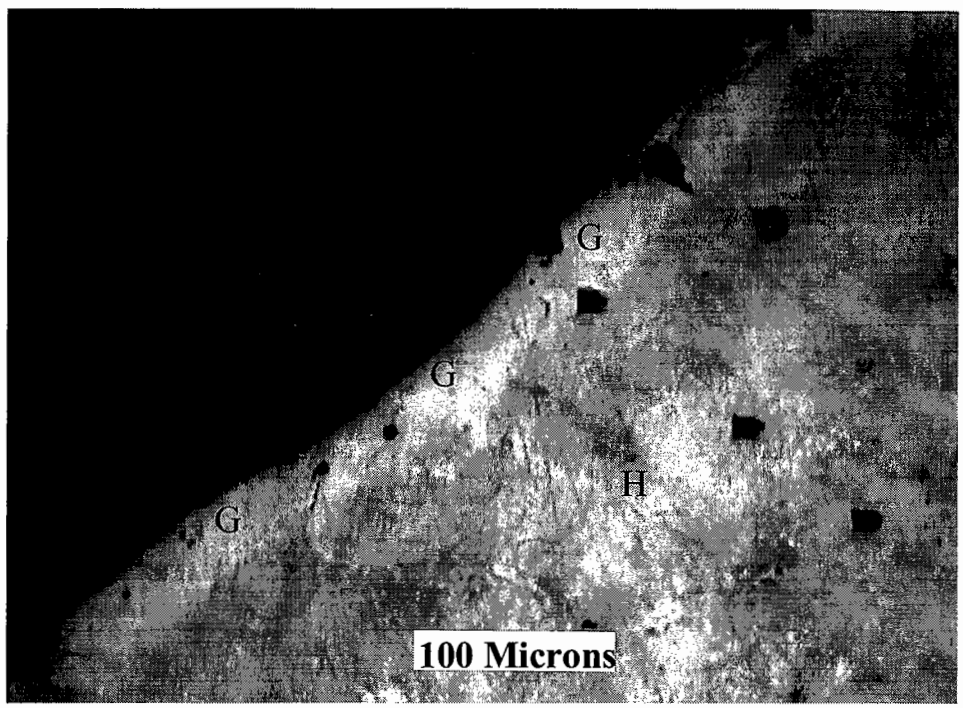

Figure 7: Microstructure of CO_2 Laser Treated Sample LB2 Near the Edge of the Laser Track. The top figure shows the substrate material (S), the heat-affected zone (H) and the "glazed" layer (G) near the edge. The bottom figure shows an enlargement of the glazed region from the other edge and the Vickers hardness impressions.

III.2. *Friction and Wear*

Fourteen friction and wear test blocks were cut from the CO_2 laser treated rail sections described previously. The samples where stamped with specimen numbers that identified the rail section and the laser track from which they were cut. The numbering scheme used a two letter prefix. The first letter, L or S, designates the rail segment as being either the long (7") or the short (3") segment, respectively (See Fig. 3). The second letter, B, W or M, designates the surface condition prior to laser treatment as either painted with black Krylon paint (B), coated with the white proprietary coating (W), or bare metal (M). Additional samples, identified with the letter V, were cut from the virgin, untreated portion of the long rail segment. In most cases, two samples were cut from each track. These samples are differentiated by the final number in the identification scheme. Table II summarizes the sample identification and gives the correspondence between the sample identification and the number that was assigned to the friction and wear test that used that sample.

Table II. Friction and Wear Sample Identification, Laser Processing Speed, and Selected Test Results

Sample ID	Rail Segment	Surface Condition Prior to Laser Treatment	Laser Processing Speed, cm/s (in./min)	Friction and Wear Test Number	Average Scar Width, mm (mils)	Calculated Scar Depth, microns (mils)	Indicated Coefficient of Friction at end of test
SB1	Short (3")	Krylon Paint	0.34 (8.0)	0104732	1.958 (77.1)	27.4 (1.08)	0.904
SB2	Short (3")	Krylon Paint	0.34 (8.0)	Not Tested	-	-	-
SW1	Short (3")	Proprietary Coating	0.42 (10.0)	0104735	2.032 (80.0)	29.5 (1.16)	1.041
SW2	Short (3")	Proprietary Coating	0.42 (10.0)	Not Tested	-	-	-
LB1	Long (7")	Krylon Paint	0.25 (6.0)	0104731	1.681 (66.2)	20.3 (0.80)	0.629
LB2	Long (7")	Krylon Paint	0.25 (6.0)	0104747	N/A	N/A	0.462
LW1	Long (7")	Proprietary Coating	0.34 (8.0)	0104733	1.886 (74.3)	26.0 (1.02)	0.939
LW2	Long (7")	Proprietary Coating	0.34 (8.0)	0104746	N/A	N/A	0.437
LM1	Long (7")	Bare Metal	0.80 (19.0)	0104741	1.489 (58.6)		0.863

Sample ID	Rail Segment	Surface Condition Prior to Laser Treatment	Laser Processing Speed, cm/s (in./min)	Friction and Wear Test Number	Average Scar Width, mm (mils)	Calculated Scar Depth, microns (mils)	Indicated Coefficient of Friction at end of test
LM2	Long (7")	Bare Metal	0.80 (19.0)	0104749	N/A	N/A	0.453
LV1	Long (7")	N/A	N/A	0104730	2.334 (91.9)	39.9 (1.57)	0.876
LV2	Long (7")	N/A	N/A	0104734	2.115 (83.3)	32.0 (1.26)	0.972
LV3	Long (7")	N/A	N/A	Not Tested	-	-	-
LV4	Long (7")	N/A	N/A	0104748	N/A	N/A	0.427

The original plan for the friction and wear tests specified that the normal loading should produce a Hertzian contact stress between the block and the ring that approximated the lateral Hertzian contact stress between a wheel flange and the rail. The AAR supplied an estimate for a typical average stress as approximately equal 190,000 psi. This is reasonably close to the average Hertzian stress of 156,000 psi at the maximum load capability of the Falex testing machine, 1,300 Lbs. It was recognized at the outset that the wear rate for the block-and-ring test would be much greater that for a rail because test geometry produces pure sliding along a single line of contact. For this reason, the temperature of the test block was continually monitored to assure that galling and welding would not occur. At the recommendation of the AAR, the test temperature was limited to the maximum temperature that has been observed in a rail after a train passes, about 150° F (70° C).

The angular velocity for the initial friction and wear tests was set at 300 RPM to approximate the sliding rate between the flange and rail surfaces during service. However, at the normal loading of 1,300 lb the wear rate in the tests was too localized and too rapid to prevent galling of both the block and the ring. Therefore, the normal loading and angular velocity of the ring were reduced until the wear rate in the virgin rail samples was such that a well-defined scar could be produced within two hours of testing. To accomplish this, the testing conditions for the first series of friction and wear tests were set at 10 lbs normal load and a ring angular velocity of 125 RPM. Although these conditions no longer match those of the rail/wheel interface, it was judged that they would be adequate for screening the differences in the friction and wear properties of treated and untreated samples. Those laser treatments that proved promising could then be applied a length of rail that could be tested under more prototypic conditions in the AAR rail/wheel testing apparatus in Pueblo, Colorado.

The first set of tests were conducted on treated samples SB1, SW1, LB1, LW1 and LM1; and virgin un-treated samples LV1 and LV2. A summary of the friction and wear measurements are given in Table II, and reproduced graphically in Figure 8. The wear values were determined from the scar width measured following the test. The values of the coefficient of friction (calculated by dividing the reaction force on the block by the applied normal force) are point values that were obtained near the end of the test at 120 minutes (7,200 s). The detailed histories of the measured coefficients of friction are shown in Figure 9. The correspondence between the test number in these figures and sample number is given in Table II.

The first thing to note from the above test results is that the treated samples generally showed a reduction in wear and friction compared to the results for the virgin rail samples LV1 and LV2. The most dramatic reduction was for sample LB2 (Table II), which, as noted previously, appeared to undergo the most surface melting. However, these test results are not necessarily indicative of the formation of an amorphous, low friction, coating on the surface. The reduced wear could be attributable to a hardened martensitic layer that is more indicative of a heat treating process than a laser glazing process. Furthermore, because of the nature of the tests, surfaces that wear more can produce artificially higher apparent coefficients of friction than surfaces that wear less. This is because of the tendency of the wear scar to accumulate debris which becomes imbedded in both the block and the ring. Visual inspection of the rings showed that this could have happened in the above tests.

Another notable feature of the preliminary test results shown in Table II and Figure 8 is the very high coefficients of friction that were measured. From prior discussions with the AAR, the coefficient of friction for dry wheel and rail conditions was expected to be in the range of 0.45 to 0.55. However, the block-on-ring tests on the virgin rail samples (LV1 and LV2) produced coefficients of friction (horizontal reaction force on the block divided by the normal force) near the end of the tests of about 0.9. If the cause of this anomalously high reading is due to debris accumulating in the wear scar, one would expect to see an increasing coefficient of friction as the tests progress. This behavior can indeed be seen in the continuous records of the coefficients of friction given in Figure 9. The first two graphs (Tests A0104730 and A0104734) are for virgin rail samples LV1 and LV2, respectively. Both figures show an increasing coefficient of friction during the test. They also show a considerable amount of scatter compared to the mean value, given by the variable 'y' in the figures. This scatter also indicates debris accumulation in the scar that, from time to time, is cleared away by the rotation of the ring. The test on the hardest laser treated sample (LB2/A0104731) shows less of an increase in the coefficient of friction, and less scatter in the data, consistent with the hypothesis that debris accumulation is the cause of both. The curves for the other laser treated samples given in Figure 9 (LW1/A0104733, SB1/A0104732, and SW1/A0104735) show a similar trend.

The sample data given in ASTM G77-93 [12] for block-on-ring tests of dry steel surfaces did not indicate that there could be a problem with debris accumulation when using this test method. The measured coefficient of friction for the ASTM tests was 0.56, which is in the range that was expected for the virgin rail tests. Consequently, the ASTM test conditions (30 lb, 197 RPM and 0.46 hour test

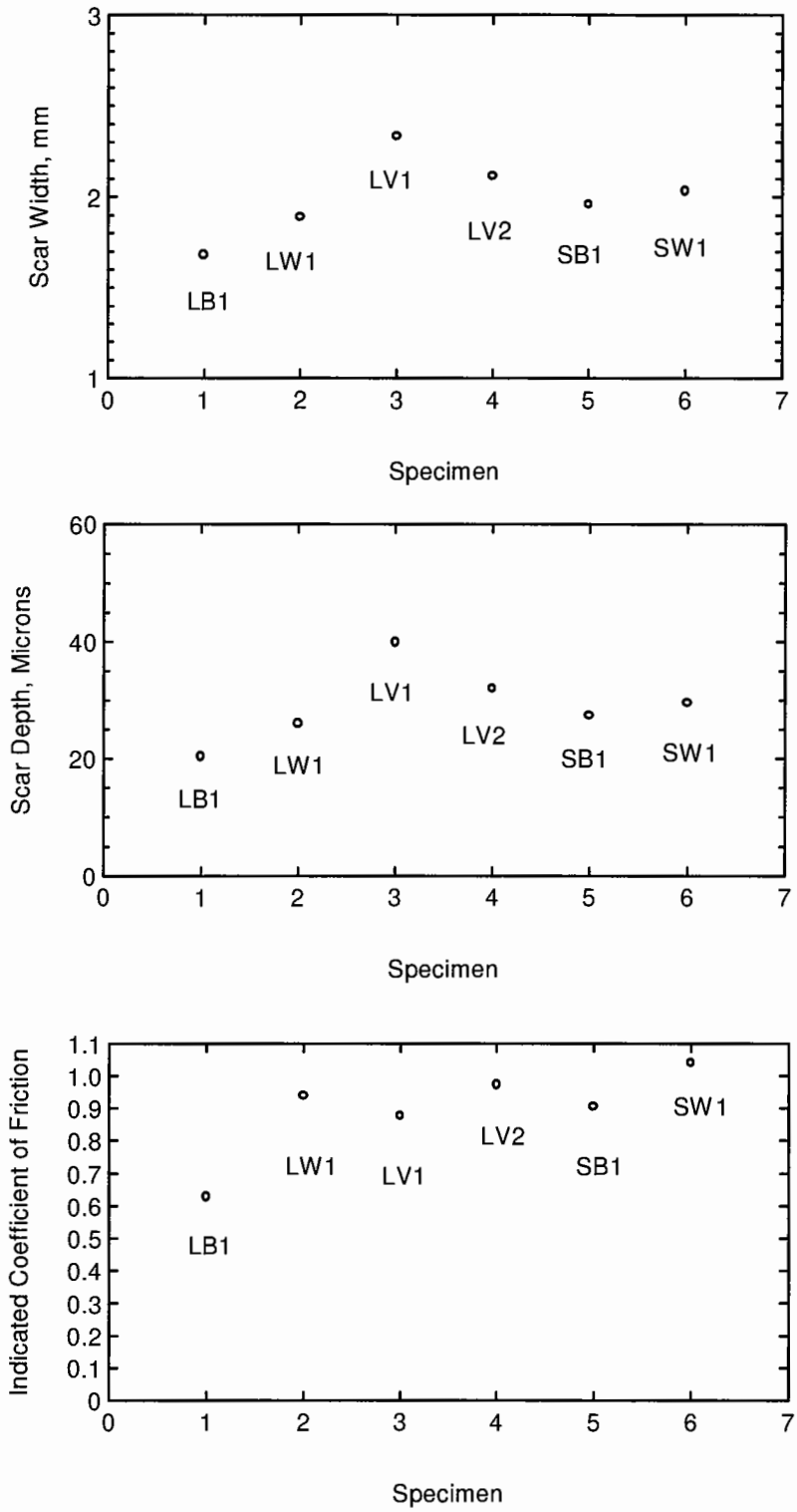

Figure 8: Friction and Wear Results for CO_2 Laser Treated Rail Samples

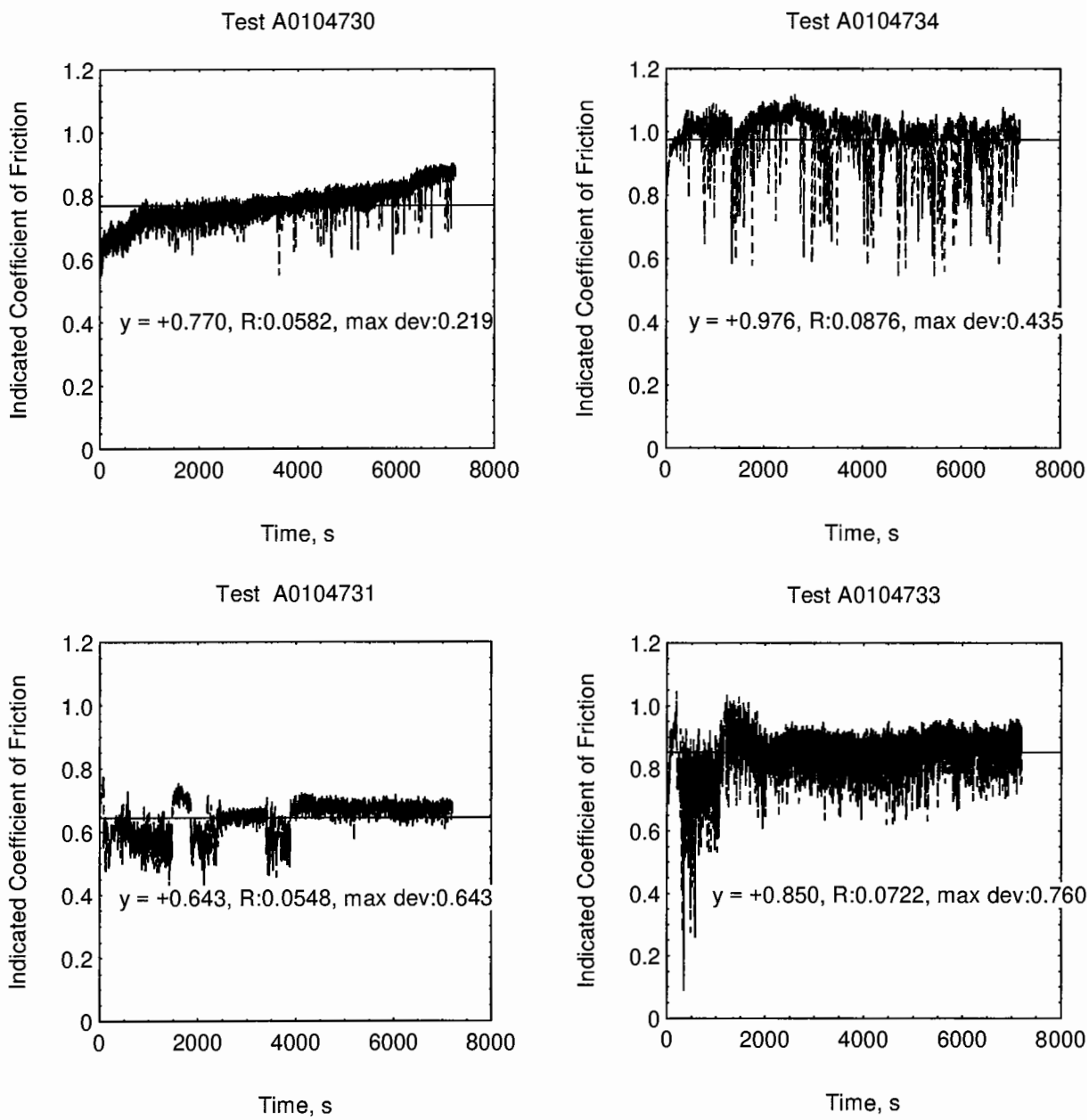

Figure 9: Continuous Records of Indicated Coefficient of Friction

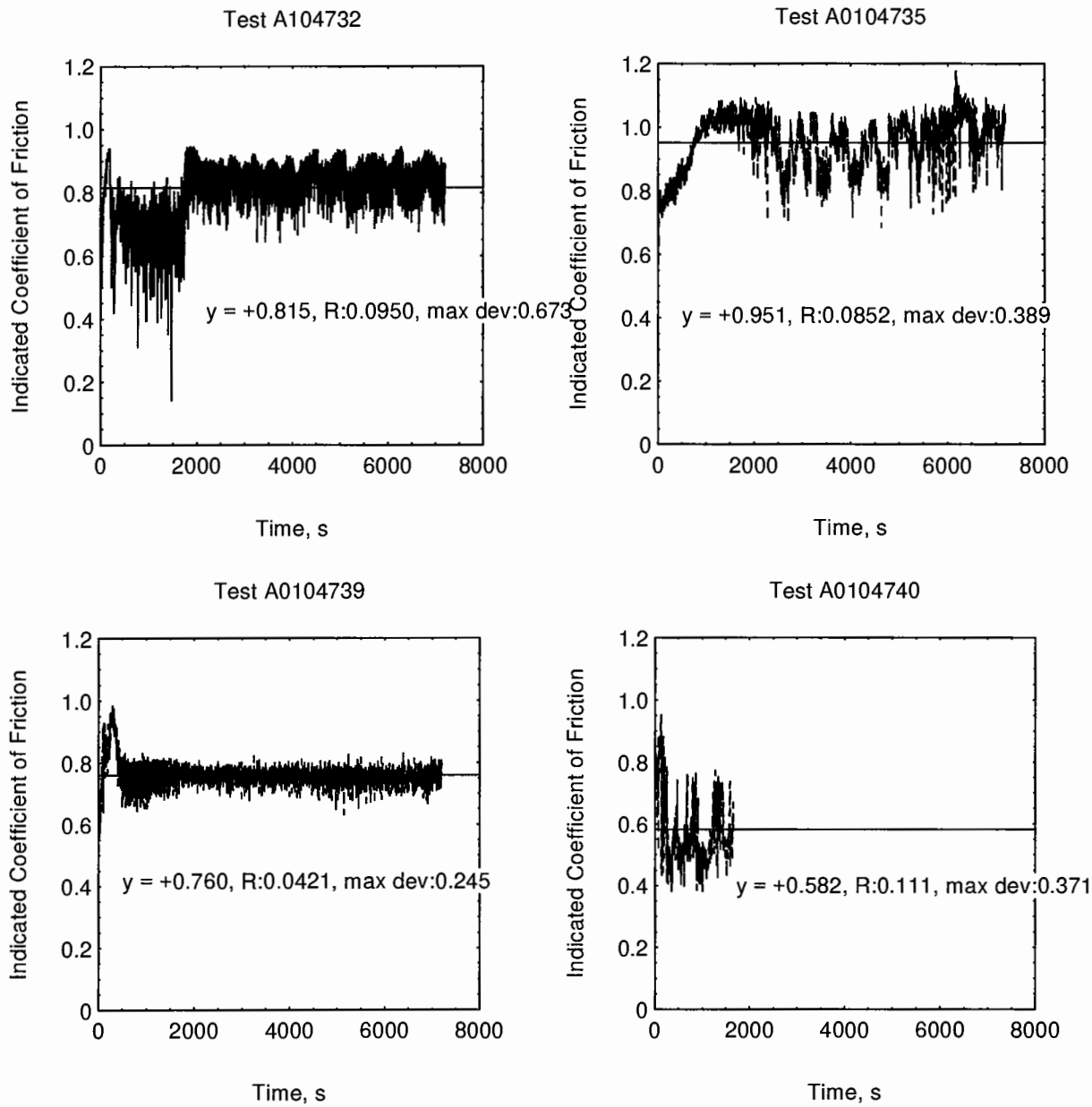

Figure 9 (Continued): Continuous Records of Indicated Coefficient of Friction

duration) and the test conditions used in the present study (10 lb, 125 RPM and 2.0 hour test duration) were repeated for the standard H-60 Falex test block (Type 01 tool steel of hardness 60 HRC) used for the ASTM data. The friction measurement for the ASTM test conditions is shown in the plot labeled A0104740 in Figure 9. The test result for the H-60 material under the conditions used for the rail tests is shown in the plot labeled A104739. It is clear from these figures that quoting a single value for the measured coefficient of friction, as is done in ASTM G77-93, is of questionable validity because it depends on the duration of the test and the instant in time where the measurement was made. The reason that shorter duration tests are likely to yield smaller values for the coefficient of friction is that the scar depth is less than for the longer duration tests.

The friction conditions at the wheel/rail interface in railroad service is such that the wear is uniform, which prevents accumulation of debris that could become imbedded in the rail or the wheel surface. This condition is similar to the condition at the friction interface in the block-on-ring tests at the beginning of the test. Therefore, it would appear that a more valid test for screening the effect of laser treatments on the coefficient of friction would be to measure the initial friction force where breakaway first occurs. The wear properties can then be measured in the same way as was done for the tests described above. Measuring the static coefficient of friction also has the advantage that the tests can be repeated for various loads, without having to worry about high local wear rates which could produce non-prototypic overheating, galling, or micro-welding of the two surfaces. A series of such tests was, therefore, performed using the second set of laser-treated rail samples that had been prepared. A sequence of loads of 100, 200, 300, 400, 500, 600, 700, 800, and 900 lbs was applied to each sample, with three runs at each load level. The motor drive on the block-and-ring test apparatus was set at 0.006 RPM, and the increase in the friction force recorded as the motor came up to speed. The results of these tests (LB2/0104747, LW2/0104746, LM2/010479 and LV4/0104748) are summarized in Table II. The coefficient of friction was calculated by dividing the maximum reaction force by the applied normal force. The maximum was clearly defined by a sudden drop in the reaction force as slipping began. The calculated coefficient of friction was also reproducible for each of the three runs at a given load, and, as would be expected, showed only a weak dependence on the magnitude of the applied normal load. Therefore, the coefficients of friction given in Table II are the average of the values for all of the runs on a given sample. This data indicates that there is no difference in the sliding resistance between the treated and untreated samples. The results are also consistent with the observation from the metallographic examinations that the CO_2 laser treatment only produced the desired surface characteristics at the edge of the tracks. The friction and wear samples were cut from the center of the tracks. Although the hardening of the surface enhanced the wear properties of the rail, it did not reduce the coefficient of friction significantly.

IV. Conclusions

The preliminary studies described here have produced promising results. They indicate that the kind of commercially available equipment housed in Argonne's Laser Applications Laboratory is suitable for modifying the surface of rail steel in ways beneficial to the railroad industry. Also, expectations based on our understanding of the relationship between the properties of surfaces produced in this way and their friction and wear behavior have been somewhat verified. A glazed microstructure was produced, particularly in the case of Nd:YAG laser treatments, with appropriate hardness and possessing a high integrity bonded interface with the substrate. Measurements of friction and wear, even for the CO_2 laser treated samples, is also encouraging of further studies. These measurements showed a marked decrease in wear with an apparent reduction in the coefficient of friction in the laser-treated samples. However, further friction testing indicated that the friction reduction may have been related to debris accumulation in the wear scar on the test blocks.

V. Future Work

V.1. *Nd:YAG Laser Treatments*

Nd:YAG lasers have many features which make them a promising, and perhaps the preferred platform, for future work. Nd:YAG lasers are reliable and simple because of their solid-state design. One of the most useful features is the ability of the Nd:YAG laser beam to be transported by fiber-optic cables. These flexible cables greatly simplify the task of getting the laser beam to the rail, especially if there are space constraints, as might be the case on a mobile rail treatment car. In addition to simplifying beam delivery, choosing the appropriate type of fiber is an important aspect of beam shaping. The optimal beam will generally have an approximately uniform irradiance. Another important reason to use Nd:YAG lasers for glazing of rails is the increased absorptivity of ferrous materials at that wavelength, which allows direct glazing without the need for an absorptive coating. Finally, the scoping tests using the Nd:YAG laser did not show the micro-cratering seen in the CO_2 tests. The use of an absorptive coating (that is not required when the Nd:YAG laser is used) may have contributed to the micro-crater formation.

There are a number of issues that need to be addressed to arrive at more definitive conclusions for laser glazing of rails. The CO_2 work was constrained by the inadequate performance of the scanner to deliver uniform illumination of the rail. The scanner has since been rebuilt to eliminate the sinusoidal intensity variations. The higher power CO_2 laser may also be necessary to produce samples with wider glazed tracks. Consequently, further tests with the improved scanner are warranted. The additional tests may also confirm or give additional insight into the cause of the micro-cratering observed.

The promising initial results obtained with the Nd:YAG laser warrant more detailed and controlled studies over a wider range of conditions, particularly prototypic conditions. If relatively large areas of the rail surface are to be glazed, it may be necessary to use multiple glazing tracks because of the power limitations. The effect of overlapping tracks on the materials properties should then be understood; overlaps in glazed areas produce a back-tempering effect and result in alternate regions of high and low friction. If the low friction areas are more wear resistant, an optimal spacing of the glazed tracks may result in equivalent performance compared to a uniformly glazed area. This method of multiple hardened tracks has been used effectively in heat treating cylinder bores of locomotive engines. The optimal glazing required may also warrant the development of special optics to deliver a more uniform Nd:YAG beam to the rail.

V.2. *Friction and Wear Measurements*

The choice of the CO_2 laser for treating the rail samples was based on the need to produce tracks from which 0.25 inch samples could be cut for block-on-ring testing. In future tests it may be possible to investigate the behavior of Nd:YAG-treated rail by taking advantage of the fact that the contact surface between the ring and the block is much narrower. However, the test results indicate that this method may not be the most suitable technique for screening the friction and wear behavior of laser-treated rail. A test method that produces a continuous wear pattern may be more desirable. This would eliminate debris accumulation in the wear scar and would allow larger loads to be applied which are more prototypic of actual rail service.

V.3. *Summary of Recommendations for Future Work*

The work described in this report has served to prove the principle that laser glazing treatments of rail steels can produce surfaces with potentially desirable properties. In our future work, we propose to conduct a focused program that will allow us to specify the parameters for laser treatments that optimize the desired surface properties, and achieve them for prototypic rail conditions.

1. We will perform a series of Nd:YAG laser treatments on flat rail steel samples to learn the conditions that will optimize achievement of desired results. This will involve:
   a. devising parameters to optimize production of the glazed microstructure across the entire width of the treated surface.
   b. engineering the conditions during melting and solidification to achieve smooth surfaces.
   c. performing microstructural examination of glazed surfaces

2. We will establish a laboratory-scale friction and wear test that:
   a. can be used to measure wear of laser treated sub-scale samples under conditions where the wear is uniform and continuous, and where the loading is more prototypic of wheel-on-rail conditions
   b. will provide reliable measurements of friction coefficients without grooving and trapping of debris

3. We will produce wider laser tracks needed for reducing friction on actual rail samples. This will involve either:

   a. laser scanning for continuous wide band laser tracks, or
   b. multiple glazing to produce parallel laser tracks spaced an optimum distance apart

4. We will demonstrate the effectiveness of promising laser treatments by

   a. performing friction testing of treated samples
   b. interacting with the AAR in preparing sections of treated rail for testing at the Transportation Technology Center in Pueblo

References

1. E. Gervais and H.J. McQueen, J. Iron and Steel Inst. March 1972, 189.
2. Jogendar Singh, JOM 44 #9 (1992) 8.
3. J.J. Gilman, J. Appl. Phys. 46 (1975) 1625.
4. Young-Won Kim, P.R. Strutt and H. Nowotny, Met. Trans. 10A (1979) 881.
5. P.R. Strutt, B.G. Lewis and Mohan Kurup, JOM 34 1982) 37.
6. J.G. Zhang, X.M. Zhang, Y.I. Lin and K. Jun, J. Mat. Sci. 23 (1988) 4357.
7. J. Singh and J.J. Mazumdar, Met. Trans. 18 (1987) 313.
8. C. Engberg and A. Blomberg, Wear 156 (1992) 121.
9. A. Bokota and S. Iskierka, Acta Met. 44 (1996) 445.
10. R.J. DiMelfi, J. Mater. Eng. 12 1990) 257
11. D.M. Follstaedt, A. Knapp and L.E. Pope, MRS Proc. 140 (1989) 133.
12. ASTM G77-93, "Standard Test Method for Ranking Resistance of Materials to Sliding Wear Using Block-on-Ring Wear Test," The American Society for Testing and Materials, Philadelphia, PA.